Peptides and metallic nanoparticles for biomedical applications

Article *in* Nanomedicine · July 2007

DOI: 10.2217/17435889.2.3.287 · Source: PubMed

6 authors, including:

Marcelo J Kogan
University of Chile
118 PUBLICATIONS **2,764** CITATIONS
SEE PROFILE

Leticia Hosta-Rigau
Technical University of Denmark
46 PUBLICATIONS **1,582** CITATIONS
SEE PROFILE

Ariel R Guerrero
None
18 PUBLICATIONS **341** CITATIONS
SEE PROFILE

Luis J. Cruz
Leiden University Medical Centre
225 PUBLICATIONS **2,692** CITATIONS
SEE PROFILE

REVIEW

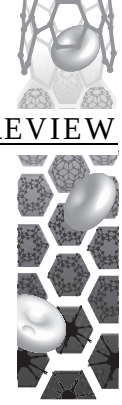

Peptides and metallic nanoparticles for biomedical applications

Marcelo J Kogan[1†], Ivonne Olmedo[1,2], Leticia Hosta[3], Ariel R Guerrero[1,4], Luis Javier Cruz[3,5] & Fernando Albericio[3,6†]

[†]Author for correspondence
[1]Departamento de Química Farmacológica y Toxicológica de la Facultad de Ciencias Químicas y Farmacéuticas, Casilla 233, Universidad de Chile, Olivos 1007, Independencia, Santiago, Chile, and Centro para la Investigación Interdisciplinaria Avanzada en Ciencia de los Materiales, Av. Blanco Encalada 2008, Santiago, Chile
Tel.: +56 2978 2897;
Fax: +56 2737 2890;
E-mail: mkogan@ciq.uchile.cl
[2]E-mail: i_olmedo@yahoo.com
[3]Institute for Research in Biomedicine, Barcelona Science Park, University of Barcelona, Josep Samitier 1–5, 08028 Barcelona, Spain
Tel.: + 34 934 034 869;
Fax: + 34 934 037 126;
E-mail: lhosta@pcb.ub.es
[4]E-mail: arielrgh@hotmail.com
[5]E-mail: jcruz@pcb.ub.es
[6]Department of Organic Chemistry, University of Barcelona, Martí i Franqués 1–11, 08028 Barcelona, Spain
Tel.: + 34 934 037 088;
Fax: + 34 934 037 126;
E-mail: falbericio@pcb.ub.es

Keywords: Au nanoparticles, biocompatibility, drug delivery, hyperthermia, *in vitro* assays, iron oxide nanoparticles, magnetic resonance imaging, nanoparticle functionalization, nanoparticle stabilization, targeting

In this review, we describe the contribution of peptides to the biomedical applications of metallic nanoparticles. We also discuss strategies for the preparation of peptide–nanoparticle conjugates and the synthesis of the peptides and metallic nanoparticles. An overview of the techniques used for the characterization of the conjugates is also provided. Mainly for biomedical purposes, metallic nanoparticles conjugated to peptides have been prepared from Au and iron oxide (magnetic nanoparticles). Peptides with the capacity to penetrate the plasma membrane are used to deliver nanoparticles to the cell. In addition, peptides that recognize specific cell receptors are used for targeting nanoparticles. The potential application of peptide–nanoparticle conjugates in cancer and Alzheimer's disease therapy is discussed. Several peptide–nanoparticle conjugates show biocompatibility and present a low degree of cytotoxicity. Furthermore, several peptide–metallic nanoparticle conjugates are used for *in vitro* diagnosis.

Nanotechnology and nanoscience studies have received much attention in the last decade. One of the major developments in these fields is the production and application of nanoparticles (NPs) in biological sciences. In general, NPs are smaller than 100 nm, contain 20–15000 atoms and are present in a realm that straddles the quantum and Newtonian scales. Metallic NPs offer a number of applications of interest in biomedicine. The size of these particles can be controlled from a few nanometers up to tens of nanometers, which places them at dimensions that are smaller than or comparable with those of a cell (10–100 µm), a virus (20–450 nm), a protein (5–50 nm) or a gene (2 nm wide and 10–100 nm long). The possibilities of these sizes imply that they could get close to a biological target of interest. When metallic NPs are magnetic, they can be manipulated by an external magnetic field gradient. This action at a distance, combined with the intrinsic penetrability of magnetic fields into human tissue, opens up many applications involving the transport and/or immobilization of magnetic NPs, or of magnetically tagged biological targets [1]. Thus, NPs can be used to deliver a cargo, such as an anticancer drug, or a cohort of radionuclide atoms to a targeted region of the body, such as a tumor. Furthermore, metallic NPs can be made to resonantly respond to a time-varying magnetic field, with advantageous results related to the transfer of energy to these particles. For example, the NP can be made to heat up, which leads to its use as a hyperthermia agent, thereby delivering toxic amounts of thermal energy to targeted bodies, such as tumors, or as a chemotherapy and radiotherapy enhancement agent, where a moderate degree of tissue warming results in more effective destruction of malignant cells. The special physical properties of magnetic NPs allow these and many other potential applications in biomedicine, such as the *in vivo* magnetic resonance detection of cancer by using multifunctional magnetic nanocrystals or the use of nanoshells (formed by a silica core covered by a thin metal shell, which is typically Au), for imaging and cancer therapy [2,3].

Metallic NPs used in therapy and diagnosis must be nontoxic, biocompatible and stable in biological media. Furthermore, they must selectively address the desired target. NPs can be coated with biological molecules to make them interact or bind to a biological target, thereby providing a controllable means of 'tagging' or targeting it. To ensure that the NP reaches the desired target, it is important to anchor a vector that specifically recognizes the target. From the point of view of molecular recognition, peptides have excellent properties that allow them to participate in ligand–receptor and protein–protein molecular interactions [4]. For instance, peptides are involved in molecular recognition of antibodies, which is relevant in the field of clinical diagnosis of infectious diseases [5] and in the design of new drugs and vaccines [6].

Mainly for biomedical purposes, metallic NPs conjugated to peptides have been prepared from Au and iron oxide (IO; magnetic NPs),

10.2217/17435889.2.3.287 ISSN 1743-5889

and there are a few examples of other magnetic NPs developed from Co. Gold nanoparticles (AuNPs) have the advantage that they present a high degree of stability and biocompatibility. By contrast, magnetic NPs are less stable and biocompatible. Capping NPs with peptides increases stability and biocompatibility and allows them to be directed to the desired target.

In the first three sections of the review, we discuss the methods for the synthesis of the building blocks required for the preparation of peptide–NP conjugates, such as AuNPs, iron oxide naoparticles (IONPs) and peptides. In the following sections, the strategies for the preparation and characterization of peptide–metallic NP conjugates are discussed. In the further sections, we address how peptides can contribute to the biomedical applications of metallic NPs. It is important to mention that several applications of these NPs have been described in the literature; however, we provide a few existent examples of the use of metallic NPs conjugated to peptides for medical applications. Finally, we draw conclusions and raise concerns that must be addressed regarding the use of these nanomaterials for biomedical purposes.

Preparation of AuNPs

Colloidal Au materials were discovered in ancient times, as reported by Daniel and Astruc [7]. Many routes to synthesize AuNPs have been described, but most start from Au (III) salts, which are then reduced to metallic Au. Almost all methods use $HAuCl_4$ as the starting reagent in H_2O. However, methods that involve other solvents are also available. The cornerstone of this process is not allowing the metallic Au nanocrystals produced to grow indefinitely. Thus, a chemical agent is added to stabilize a AuNP. Given the small sizes of the crystals, the interface between these and their medium is large and, therefore, the surface exposed is also extensive. Stabilizing agents lower interfacial tension by covering the surface of the NP, thereby forming a monolayer. This cover is sometimes called capping, a key point in the synthesis of NPs since it determines the stability of these molecules. The resulting system has the properties of a lyophobic colloidal dispersion of metallic Au, rather than those of a dissolution. However, if there is enough dispersant, the colloid is transparent and resembles a dissolution.

Since crystallization cannot be controlled easily, the resulting AuNPs are not uniform in size. Therefore, the size dispersion obtained is analyzed by a number of microscopy techniques, such as transmission electronic microscopy (TEM), scanning electronic microscopy (SEM) and atomic force microscopy (AFM). Variations in size and size dispersion are obtained in function of the reducing reagent and technique used. In recent years, several external-aid techniques have been used to achieve an improved control of size dispersion. These techniques are described briefly below.

The classical sodium citrate reduction is one of the oldest methods, and is by far the most widely used. It was first described by Turkevich and colleagues in 1951 [8]. In essence, it consists of an aqueous $HAuCl_4$ reduction with trisodium citrate as the reducing and stabilizing agent. The resulting NPs acquire a citrate layer over their surface, which confers stability. However, citrate can be easily displaced by several species that form stronger interactions with Au. TEM has shown that these NPs are approximately 20 nm and show little dispersion. Later, it was discovered that size can be controlled by changing the $HAuCl_4$:citrate ratio [9]. NPs could be conjugated with peptides directly conjugated with a Cys or a bifunctional linker.

In addition, AuNPs can be prepared by reduction of $HAuCl_4$ using a surfactant method. In this technique, the surfactant forms micelles, which stabilize the NPs. In this case, reduction reagents stronger than citrate are usually applied, such as $NaBH_4$. Many surfactants have been used for this purpose, most of which are quaternary ammonium salts, such as cetyltrimethylammonium bromide (CTAB) and, recently, didodecyldimethylammonium bromide (DDAB) [10] and tetradodecylammonium bromide (TTAB) have also been described [11]. Anionic surfactant syntheses are less frequent, but a number have also been reported [12].

The resulting NPs usually have smaller mean sizes than their citrate counterparts, although they have broader size dispersion, unless a seeding procedure is used. In this procedure, smaller NPs (usually less than 6 nm in diameter) are synthesized first, and they are known as seeds. Later, these seeds are grown under another $HAuCl_4$-reduction stage [13]. AuNPs can be stabilized by thiols and other sulfur compounds. In this case, the NPs are obtained with a strong reducing agent, as in the previous method, but the strong interaction between sulfur and Au allows thiol compounds to form a self-assembled monolayer (SAM) adsorbed over the NP surface, thereby conferring the NPs increased stability.

In recent years, several new techniques using an external energy source have been tested. These offer several advantages and disadvantages compared with traditional techniques. Microwaves have been applied to increase the solvent temperature via microwave irradiation [14,15]. In this case, a slightly narrower size range is achieved. This technique is also faster than the typical reflux apparatus used in classical citrate reduction. In one of the methods described, a microwave oven is modified to obtain reflux. In addition, laser irradiation can be used through direct ablation of a metallic Au surface [16] or to control the standard reduction of $HAuCl_4$ [17]. In the former case, no reduction is performed, the process is completely physical and laser simply destroys a Au bulk material leaving Au nanosized pieces. The resulting particles show more irregular shapes, as shown by TEM micrographs. The ultrasound technique is used to generate H and hydroxyl radicals. Similar to traditional methods, ultrasound methods start from Au salts, but H radicals are used as the reducing agents and a range of sizes and shapes are obtained [18–20]. X-ray and γ-ray radiation have also been applied for the preparation of Au colloids [21,22] and have achieved efficient yields and small size dispersions, without requiring heat. The reduction mechanisms for x- and γ-rays have been studied by Karadas and colleagues [23] and Gachard and colleagues [24], respectively.

AuNPs can be stabilized with biological molecules. The recent findings for the biological applications of these particles have introduced the need for biocompatibility. In this case, the main concern is the outer capping, which can make NPs toxic *per se* or nontoxic. This capping can also enhance rejection by the immune system.

Laser-ablation synthesis has been used to stabilize AuNPs with known biocompatible molecules, remarkably, cyclodextrins, 3-mercaptopropionic acid and *N*-propylamine [25]. In this study, the authors note that traditional chemical techniques require the presence of toxic by-products, therefore, laser ablation and x-rays are proposed as alternatives for the synthesis of biocompatible NPs. However, another recent study describes a simple synthesis using isoascorbic acid as a reducing reagent [26], which appears to be a promising candidate for biologically compatible NP dispersions. Another possibility is simply to synthesize NPs with one of the methods described above and later functionalize them with known biomolecules. This method will be described later.

Preparation of IONPs

The synthesis of magnetic NPs with customized sizes and shapes remains a scientific and technological challenge. IONPs have been used for biomedical purposes for 40 years and several studies have addressed this subject. The preparation of these NPs has been reviewed recently by Gupta and Gupta [27]. Physical methods, such as gas-phase deposition and electron beam lithography, are elaborate procedures that have the disadvantage that the size of particles in the nanometer range cannot be controlled. The wet chemical routes for the preparation of magnetic NPs are simpler, more tractable and efficient and allow appreciable control over size, composition and sometimes even the shape of the particles.

IONPs (either Fe_3O_4 [magnetite] or γ-Fe_2O_3 [maghemite]) can be synthesized through the co-precipitation of Fe^{2+} and Fe^{3+} aqueous salt solutions by the addition of a base [28]. The control of size, shape and composition of NPs depends on the type of salts used (e.g., chlorides, sulphates, nitrates or perchlorates), the Fe^{2+} and Fe^{3+} ratio, pH and ionic strength of the media [29,30]. Furthermore, the precipitation to obtain the particles can be performed in constrained domains. Advancement in the use of magnetic particles for biomedical applications depends on the development of new synthetic methods with better control over NPs size distribution, magnetic properties and surface characteristics. Organized assemblies [31] or complex structures have been used as reactors [32] to obtain ultrafine magnetic IONPs. Stable aqueous magnetic suspensions can also be prepared using various saturated and unsaturated fatty acids as primary and secondary surfactants [33]. In practice, however, little control can be exercised over the size and size distribution of the nanostructures. Moreover, owing to the constraints of low reagent concentrations required by this synthetic procedure, only small amounts of IONPs can be obtained. A variety of other methods based on the principle of precipitation in highly constrained domains have been developed; these include sol–gel preparation [34], polymer matrix-mediated synthesis [35] and precipitation using microemulsions [36] and vesicles [37]. Small amounts of IONPs have been produced in apoferritin cages and laboratory-grown bacteria [38].

Peptide synthesis

Although several methodologies have been described for peptide synthesis [39], the one of choice for the preparation of peptides to be

linked to NPs is the solid-phase technique, introduced by Merrifield in the 1960s [40]. Due to its simplicity, this method can be performed by nonspecialist chemists for the synthesis of short peptides. Solid-phase peptide synthesis (SPPS) is based on linking the first amino acid of each sequence onto a solid support that is insoluble and inert to all the reagents and solvents used in the synthesis. SPPS is carried out in a single reactor, reactions are driven to completion by using large excess of the soluble reagents and excess of reagents and all soluble side products are removed by filtration and washings. After the incorporation of the first amino acid, a recurrent synthetic protocol is applied, which consists of the addition of a new residue at each time point. The α-amino group and lateral side chains are protected to prevent possible side reactions. For the incorporation of each amino acid, the carboxyl function must be activated. This is performed by using carbodiimides in the presence of *N*-hydroxybenzotriazoles or stand-up coupling reagents, such as uronium/aminium or phosphonium salts [41]. After coupling, the extent of the coupling is verified by a colorimetric test, the ninhydrin test being the most convenient. If this test is positive (presence of free amines), the coupling is repeated until the reaction is completed [42]. At the end of the synthetic process, the peptide is released from the resin. Figure 1 shows the SPPS methodology.

The most convenient chemical SPPS strategy is the so-called fluorenylmethyloxycarbonyl (Fmoc)/*tert*-butyl (*t*Bu) [43]. Thus, Fmoc, which is removed by means of piperidine through a β-elimination reaction, masks the α-amino function, and trifluoroacetic acid (TFA) labile groups, such as the *t*Bu, trityl (Trt) or activated sulfonyl, are used for the side-chain functions. When possible, peptides are synthesized in the form of a C-terminal amide using, for instance, a Rink amide resin. This resin is highly convenient because the incorporation of all amino acids is

Figure 1. Solid-phase peptide synthesis strategy.

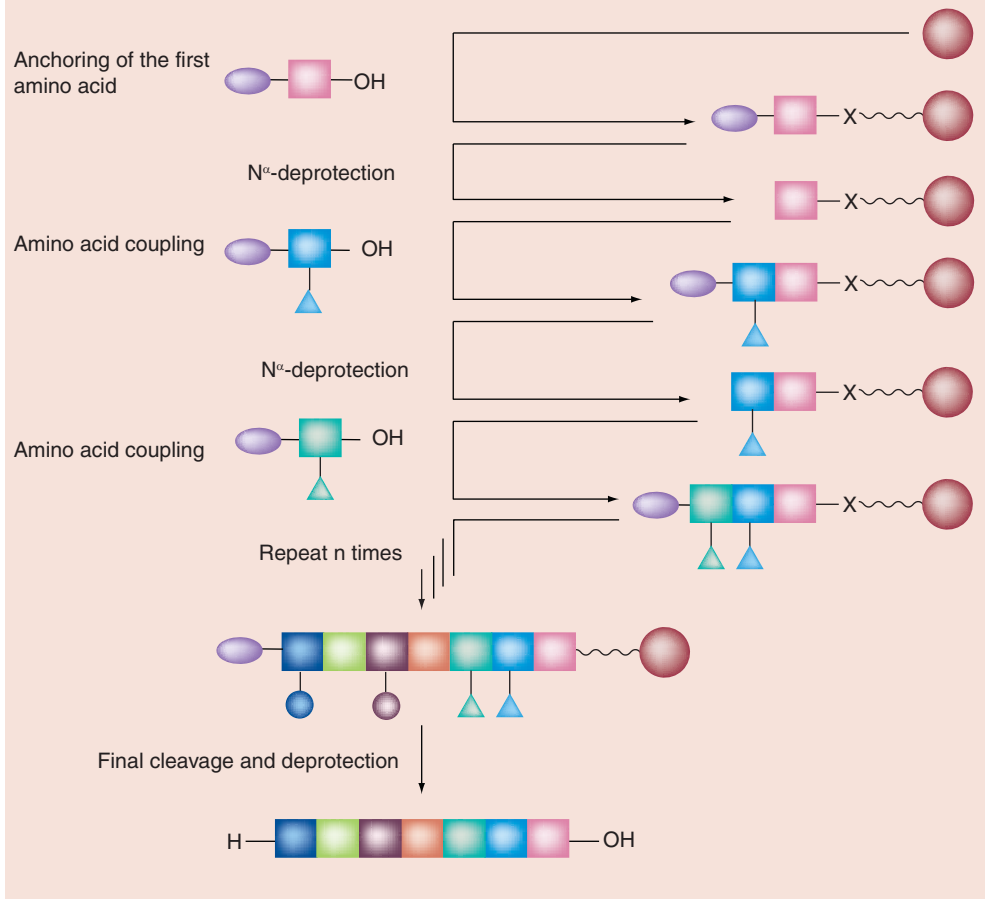

Figure 2. Two strategies for the preparation of peptide–Au nanoparticle conjugates.

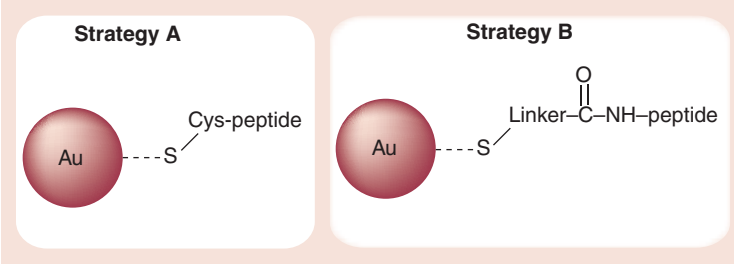

carried out through the formation of an amide/peptide bond. When C-terminal acid peptides are required, the chloro-2-chorotrityl resin (CTC or Barlos resin), which can release the peptide even in the presence of a low TFA concentration solution, is recommended.

For the preparation of the peptide–AuNP conjugate following strategy A (Figure 2), the peptide is linked to the AuNP by a thiol group, which can be present in the peptide through a Cys residue. The peptide is synthesized using a Cys protected with Trt, which is removed during the final cleavage from the resin. The Trt group also serves to protect the thiol group present in the bifunctional linker through a carboxyl group held in the linker. This Cys-protected amino acid is usually incorporated at the end of the stepwise elongation at the N-terminal [44]. If necessary, peptides can be purified by high-performance liquid chromatography (HPLC) before incorporation to the NPs [45].

Preparation of peptide–metallic NP conjugates

Two main strategies to bind peptides to AuNPs have been reported. In strategy A, the conjugation of a peptide with biological activity to a AuNP is by means of the spontaneous reaction of a thiol (present in a Cys moiety belonging to the peptide sequence) (Figure 2, Strategy A) with the AuNP surface. Thiols are the most important type of stabilizing molecule for AuNPs of any size. It is an accepted assumption that the use of thiols leads to the formation of strong Au–S bonds [46].

One example of this kind of conjugation is the binding of the peptide CLPFFD (Cys–PEP) to the Au surface, as recently reported by our group [47]. Other examples include the conjugation of CALNN peptides, reported by Levy and colleagues [48–50]. By contrast, in strategy B, a functionalized NP is capped with a linker, which is then activated and functionalized with the biologically active peptide. The linker is a bifunctional molecule containing a thiol, which allows binding to the Au surface, and a functional group (e.g., carboxyl group), which is bound to the peptide. One example of this strategy is the functionalization of AuNPs with tiopronine and the conjugation of these functionalized NPs with the peptide GRKKRRQRRR [51].

In the case of IONPs, they are first stabilized with an adsorbed layer of a biocompatible polymer, such as dextran or polymetacrylate, and the peptide is then conjugated with the biocompatible IONPs (Figure 3) [27].

Various biological molecules, such as antibodies, proteins, peptides and targeting ligands, can also be bound to the polymer surfaces on the NPs by chemical coupling via amide or ester bonds to make the particles target specific. Linker molecules, such as *N*-succinimidyl 3-(2-pyridyldithio) propionate (SPDP), *N*-hydroxysuccinimide or *N*,*N*´-methylene-bisacrylamide (MBA), are commonly used to attach the peptide molecules to the polymer surface on the NPs [52]. Ligands, such as the Tat sequence (which enhances intracellular delivery) [53,54] and RGD (which increases cell spreading and differentiation and enhances DNA synthesis), have been attached to IONPs (Figure 4).

Characterization of peptide–metal NP conjugates

The characterization of metallic NPs is an extended field that is out of the scope of this review. Our attention is focused on the techniques that allow the characterization of peptide–metal NP conjugates. The characterization of conjugated peptide–AuNPs requires the use of

Figure 3. Biocompatibilization of iron oxide nanoparticles.

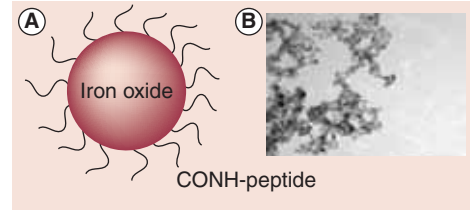

(A) An iron oxide nanoparticle capped with a biocompatible polymer and functionalized with a peptide. **(B)** Transmission electron microscopy micrograph ofiron oxide nanoparticles biocompatiblized with polymetacrylate. The diameter is 8 ± 2 nm.
(Kogan MJ *et al.* Unpublished Data).

Figure 4. Triple-label cross-linked iron oxide nanoparticles–Tat.

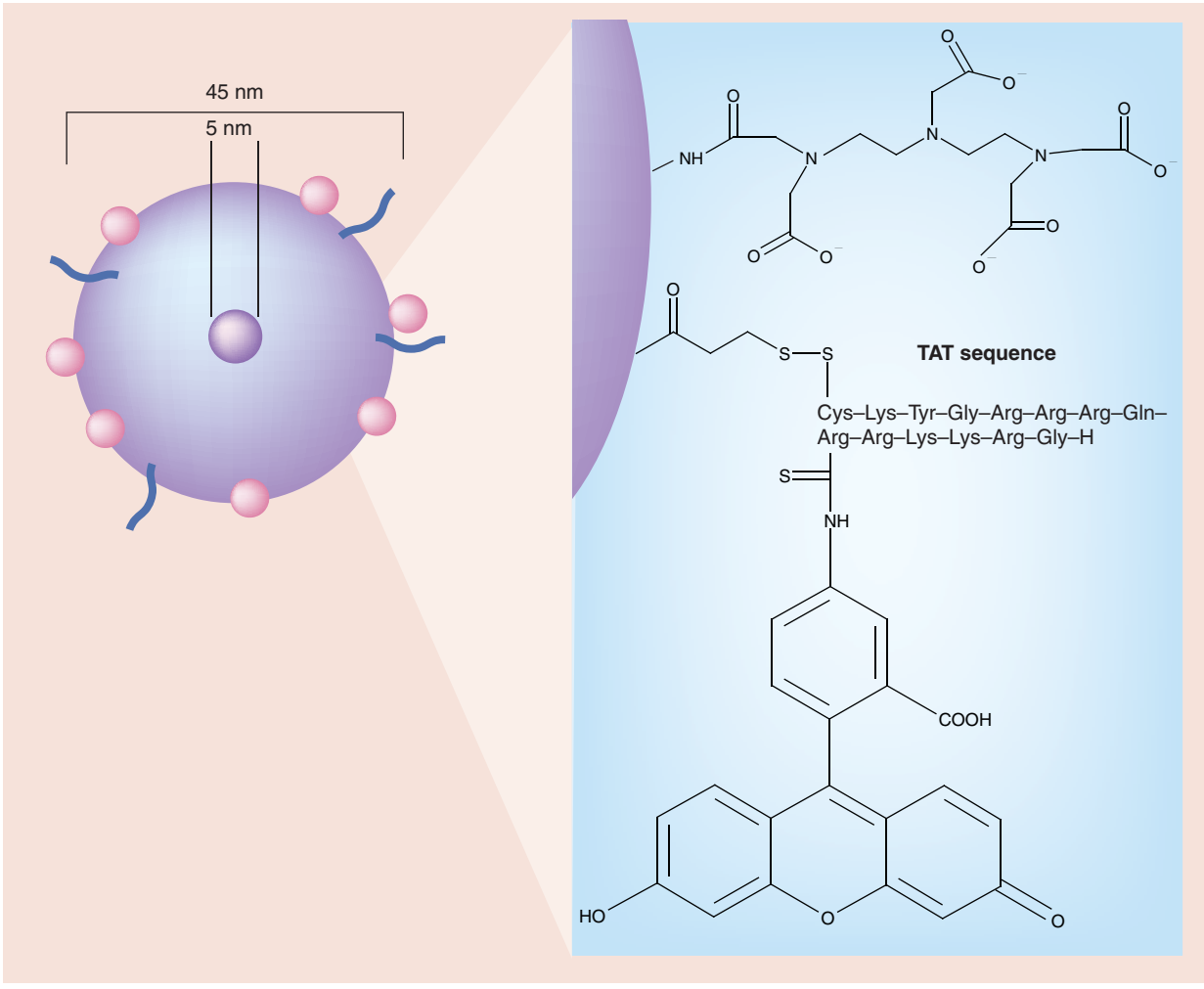

The magnetic particle developed consists of a central superparamagnetic iron oxide core (dark purple core) sterically shielded by cross-linked dextran (purple). The particle core measures approximately 5 nm and the overall particle size is 45 nm. The fluorescein isothiocyanate-derivatized Tat peptide (blue) was attached to the aminated dextran, thereby yielding an average of four peptides per particle. The dextran surface was also modified with the chelator diethylene triamine penta-acetic acid (pink) for isotope labeling. Modified from [53].

combined approaches. A preliminary evaluation of the conjugation can be performed using techniques such as ultraviolet (UV)-vis spectroscopy. This technique provides information concerning NP capping. Several procedures, such as x-ray photoelectron spectroscopy (XPS), can be used to characterize and determine the presence of Au–S bonds. Vibrational spectroscopy methods, such as infrared (IR) spectroscopy, are well suited for the detection of chemical bonds. In addition to the spectroscopic techniques, TEM and dynamic light scattering (DLS), which allows determination of the size, shape and aggregation state of the conjugates, have been described. Furthermore, other useful approaches are available, such as amino acid analyses combined with HPLC, which allows the determination of the ratio of peptide molecules per NP. Furthermore, zeta potential measurements give an idea of the surface charge around the NPs. The next section provides a brief description of these techniques and representative examples are provided.

AuNPs display optical properties that could be exploited in optoelectronic devices [55]. The source of the optical absorption is the surface plasmon resonance (SPR). Small shifts in the position of the SPR occur as a result of changes in the dielectric properties of the medium in which the Au particles are found or the presence of materials adsorbed on the surface of the Au particle. Mie's

scattering theory is frequently used to explain shifts in SPR [56–58]. The theory predicts that shifts in this resonance can also occur when particles deviate from spherical geometry. In this scenario, the transverse and longitudinal dipole polarizability no longer produces equivalent resonances. Consequently, two plasmon resonances appear, a broadened and red-shifted longitudinal resonance and a transverse resonance whose absorbance remains centered around 540 nm [59,60]. Aggregation causes coupling of the plasma modes of AuNPs, which results in a red shift and broadening of the longitudinal plasmon resonance in the optical spectrum [61]. Mandal and Sin have systematically studied the effect of pH on the assembly/disassembly of carboxylated peptide-functionalized AuNPs (peptide–AuNPs) driven by H-bond interactions [62]. The peptide–AuNPs show a characteristic SPR band at 527 nm with an average particle size of 8.7 nm. Figure 5 shows a set of UV-vis spectra with a change in the SPR band of peptide–AuNP suspensions at various pH values (viz., 2, 2.5, 3, 3.5, 4, 4.5 and 6–7) taken 15 min after acidification of the medium occurs. The change in the SPR bands indicates that aggregation of the AuNPs differs depending on the pH.

Figure 5. UV-vis absorption spectra of peptide–Au nanoparticles at a range of pH values taken 15 min after the adjustment of the respective pH values.

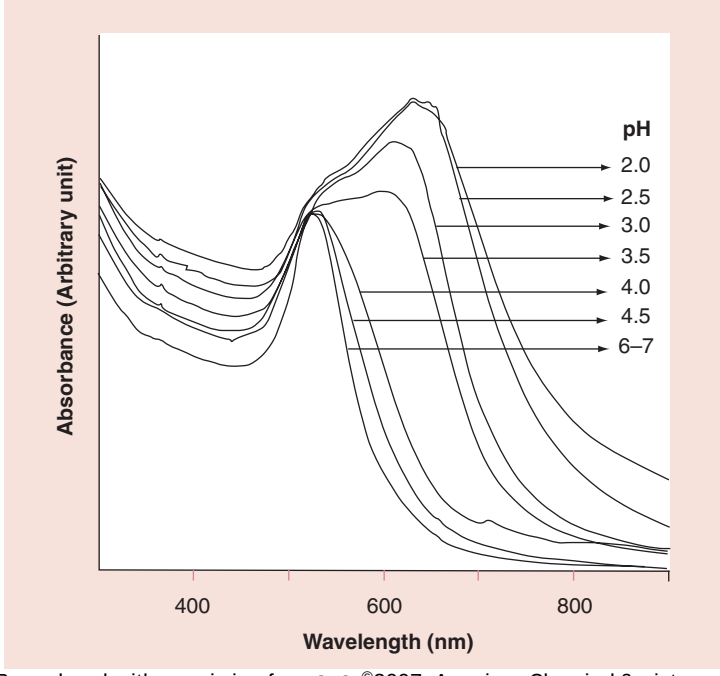

Reproduced with permission from [62]. ©2007, American Chemical Society.

An example of the shift of the SPR band was reported by Kogan and colleagues [47]. These authors observed that the conjugation of AuNPs with Cys–PEP produces a red shift in the SPR of the colloidal AuNPs (from 519 to 527 nm when Cys–PEP is attached to the AuNPs). The small shifts in the position of the SPR occur as a result of the presence of the peptides adsorbed on the surface of the AuNPs. By contrast, UV-vis spectroscopy is useful to determine the stability of the conjugates in a range of ionic strengths and pHs. Levy and colleagues studied the stability of AuNPs capped with the peptide CALNN and defined the aggregation parameter to evaluate stability in distinct conditions [48].

The size, shape and aggregation state of NPs can be determined by TEM. An example of this characterization is the study published by De la Fuente and colleagues, who reported the synthesis of water-soluble AuNPs functionalized with the Tat protein-derived peptide sequence [63]. Figure 6 shows the TEM image and core size distribution histogram of these AuNPs.

Tkachenko and colleagues synthesized peptide–AuNP complexes [64,65]. These were assembled by conjugating peptides to bovine serum albumin (BSA) and then attaching BSA–peptide conjugates to AuNPs. The capped AuNPs were observed by TEM. A low electronic density was observed around these particles (Figure 7). In addition, BSA–peptide conjugates to AuNP were analyzed by DLS. DLS and TEM together revealed that these conjugates add 4 nm to the hydrodynamic diameter of the particle.

XPS is a powerful technique widely used for the surface analysis of materials. At low energy resolution, it provides qualitative and quantitative information on the elements present, while at high energy resolution, it gives data on the chemical state and bonding of these elements. In the XPS technique, x-ray photons of a well-defined energy hit the sample and eject photoelectrons from the atomic core level and valence levels. A computer-based data system helps to differentiate the electron energies and accumulates counts of the electrons detected, hence generating a photoelectron spectrum. The data system is also used for subsequent manipulation of spectra, such as element identification, quantification, curve fitting and plotting. The x-rays penetrate several micrometers (1–3 µm) into the sample, thereby producing photoelectrons throughout the penetration depth of the rays. The energy of the photoelectrons emitted is

Figure 6. Transmission electron microscope micrographs and core size distribution histograms (inset) of AuNP–tiopronin nanoparticles.

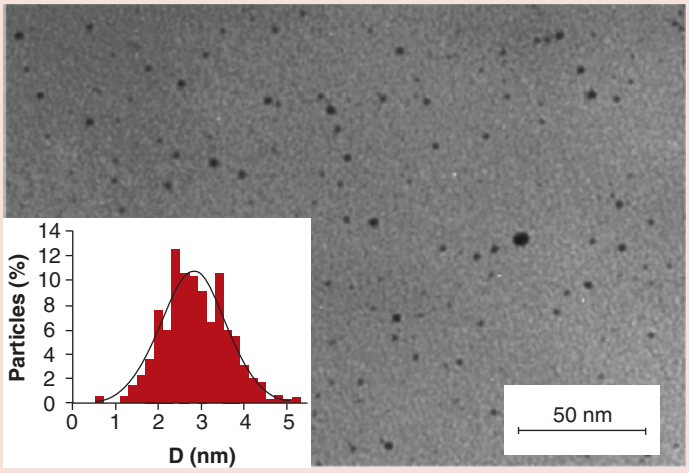

Reproduced with permission from [63]. ©2005, American Chemical Society.

characteristic of their original electronic states, which include bonding state information. The photoelectrons that escape into the vacuum are collected, their energy resolved, slightly retarded and counted, which results in a spectrum of electron intensity as a function of the measured kinetic energy. The kinetic energy values, which are source dependent, are converted into binding energy (BE) values, which are source independent. The binding energies of the electrons measured are characteristic of the chemical structure and bonding of the material. By comparing the experimentally measured BE values with those available in various reference sources, the chemical nature, state or species of the surface can be determined. Several examples of the use of XPS for characterizing peptide-coated AuNPs can be found in the literature [66]. Another example of XPS for the characterization of AuNP conjugates was described by Kogan and colleagues [47]. AuNPs were linked to the peptide Cys–PEP, thereby forming the conjugated AuNP–Cys–PEP. The relative intensity of the Au peaks indicated that approximately 20–25% of Au atoms shift to higher energies. This shift would correspond to the atoms bound to the Cys at the surface layer of the particle.

The preparation and properties of a series of Au nanoclusters protected by thiolated peptides based on the aminoisobutyric acid (Aib) unit have been described by Fabris and colleagues [67]. AuNP–peptide conjugates were characterized using XPS. For all samples, signals from Au, C, O, N and S were obtained and no other elements were detected. The Au4f level was characterized by a sharp doublet with a peak-to-peak separation of 3.6 eV. Within the series of peptides bound to the AuNP series, the BE of the Au4f7/2 peak was fixed to 84.0 eV, which is the typical value expected when thiolate monolayers self-assemble onto Au nanoclusters or extended Au surfaces [68,69].

Together, XPS, UV-vis spectrophotometry, analysis of amino acids (which determines the amino acid composition of a peptide or protein) and HPLC allow the determination of the number of peptide molecules per AuNP. This number can be estimated by combined techniques. The concentration of NPs in the solution (before conjugation) can be determined by reading the absorbance at the peak (in the case of 10-nm AuNPs it is 520 nm) and taking into account molar extinction coefficient [70].

After conjugation, the peptide is separated from the free fraction by centrifugation of the conjugates. An analysis of the amino acids of the AuNP–peptide pellet then allows the determination of the amount of peptide attached to the Au surface. For amino acid analysis, the peptide is normally hydrolysed in 6N HCl. The free amino acids are then derivatized with phenylisothiocyanate to produce phenylthiocarbamyl (PTC) amino acids. The derivatized amino acids are separated on a C_{18} reversed-phase column with an acetonitrile gradient in NaAcO buffer. Alternatively, amino acids can be separated by ionic-exchange chromatography and detected by reaction with ninhydrin.

In order to confirm the presence of peptide in the pellet formed by the AuNP–peptide complex, Kogan and colleagues performed an amino acid analysis of the AuNP–peptide pellet obtained after centrifugation of the conjugates [47]. The free fraction of the peptide (i.e., the nonconjugated peptide) was determined by HPLC and the conjugated peptide was estimated by difference.

NPs are also characterized by zeta potential measurements. Zeta potential refers to the electrostatic potential generated by the accumulation of ions at the surface of a (colloidal) particle that is organized into an electrical double layer consisting of the Stern layer and the diffuse layer. Zeta potential is a measure of the magnitude of the repulsion or attraction between particles. Its measurement provides a detailed insight into the dispersion mechanism and is the key to

Figure 7. Transmission electron microscope image of a bovine serum albumin–peptide conjugate.

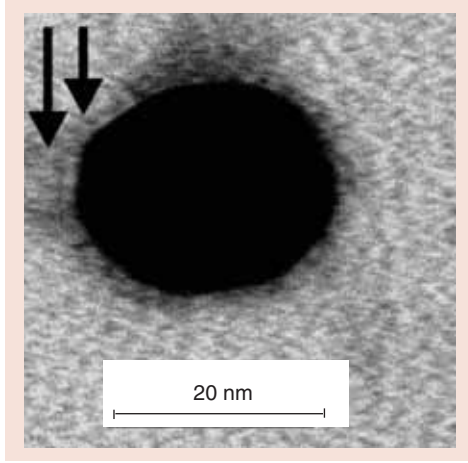

The arrows indicate an increase of approximately 2 nm around the radius of the Au nanoparticle. Reproduced with permission from [64]. ©2004, American Chemical Society.

electrostatic dispersion control. By measuring fundamental parameters, such as the zeta potential, particle size, pH and conductivity, it is possible to estimate the stability of the colloidal solution. Slocik and colleagues used several peptides to obtain monodisperse and stable AuNPs [71]. In their study, the presence of the surface-adsorbed peptides was confirmed by zeta potential measurements and by fourier transform IR (FT-IR) spectroscopy. The results of the latter showed distinctive vibrations that arise as a result of the surface-constrained peptides on the AuNPs.

Biomedical applications of peptide–AuNP conjugates

The labeling of targeting molecules with NPs has revolutionized the visualization of cellular or tissue components *ex vivo* and *in vivo* by electron microscopy. In this regard, De La Fuente and Berry synthesized AuNPs functionalized with the Tat protein-derived peptide sequence GRKKRRQRRR in order to transport the NPs to the cell nucleus [63]. AuNPs were first protected with the nonamino acidic tiopronin and then functionalized with the peptide sequence, thereby obtaining two types of NPs, AuNP–tiopronin and AuNP–Tat (Figure 8). To compare their capacity to enter the cell, the two NPs were incubated with hTERT-BJ1 human fibroblasts. TEM images showed that both NPs were taken up into the cell, but only a few AuNP–tiopronin NPs were taken up through membrane invaginations and accumulated in the mitochondrial surrounding. By contrast, AuNP–Tat particles were located mainly in the nucleus since they had a nuclear-localization sequence and were small, which allowed them to penetrate the cell membrane and target the nucleus. The authors also performed toxicity studies using a 3,4,5-dimethylthiazol-2-yl-2,5-diphenyl tetrazolium bromide (MTT) assay in the same cell line. The metabolic activity and proliferation of fibroblasts were measured after 24 h of culture. No appreciable cytotoxic effects were detected [63].

De la Fuente and colleagues also synthesized AuNPs using several alkanethiolate capping agents [51]. These AuNPs were derivatized with two distinct diamine-functionalized linkers, ethylenediamine (EDA) and bis (3-amino-propyl) poly(ethylene glycol) (PEG), plus the GRGDSP peptide sequence. These authors used two methods to obtain AuNPs. In the first, NPs were prepared by adding either an aqueous solution of L-cysteine or a methanolic solution of 11-mercaptoundecanoic acid (MUA) to an aqueous solution of $HAuCl_4$, followed by reduction with $NaBH_4$ to obtain AuNP–cysteine and AuNP–MUA. Alternatively, codissolution of $HAuCl_4$ and tiopronin in a MeOH/HOAc mixture gave a stable ruby-red solution, which, by $NaBH_4$ reduction, provided AuNP–tiopronin as a dark solution. These NPs were modified with EDA and PEG, thereby obtaining AuNP–tiopronin–EDA and AuNP–tiopronin–PEG, which were then functionalized with the GRGDSP peptide to target integrins on the cell surface and evaluate parameters such as stability, biocompatibility and cytotoxicity. Cell viability was evaluated by the MTT assay in hTERT–BJ1 human fibroblasts. Proliferation and metabolic activity was thus measured after a 24-h culture. Cell viability was more favorable for coated NPs (AuNP–tiopronin–EDA and AuNP–tiopronin–PEG) than for uncoated ones. At concentrations up to 2.5 µM, the AuNP–tiopronin–RGD conjugate did not have cytotoxic effects on fibroblasts. At concentrations higher than 2.5 µM, AuNP–tiopronin–RGD and AuNP–tiopronin–PEG–RGD conjugates affected metabolic activity, although, below this concentration, this activity did not change in comparison with controls. SEM images of cell morphology in response to particle incubation taken at 24 h showed that each NP type with different surface characteristics caused a distinct cell response (Figure 9). Thus, incubation with AuNP–tiopronin–RGD produced large aggregates, probably due to the interactions between the carboxyl

Figure 8. Preparation of AuNPs–Tat.

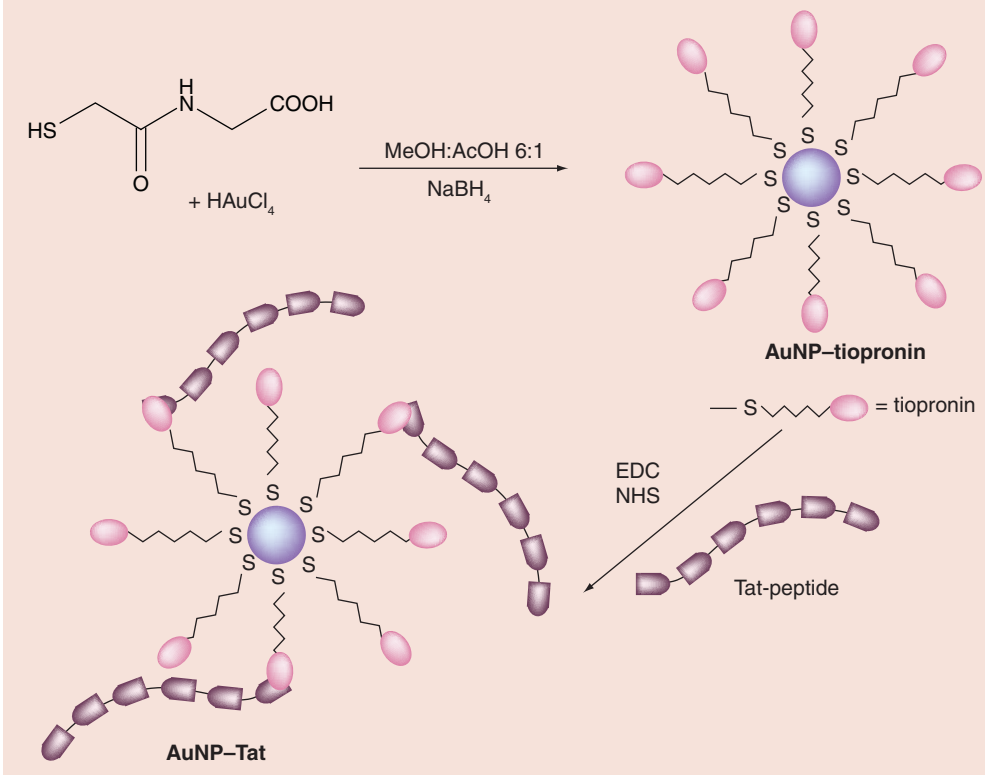

EDC: 1-ethyl-3-(3-dimethylaminopropyl)-carbodiimide; NHS: *N*-hydroxy-sulfosuccinimide; NP: Nanoparticle. Modified with permission from [63].

groups on the surface of the NP with culture medium proteins. Cells reacted strongly with the AuNP–tiopronin–EDA–RGD conjugate, forming lamellipodia and filopodia on the cell membrane. Moreover Au–tiopronin–EDA–RGD conjugates were internalized via endocytosis. Although these NPs cannot be considered a system for cell labeling, they may be useful as internalization vehicles, particularly given their low toxicity, even at high concentrations. Regarding AuNP–tiopronin–PEG–RGD conjugates, as a result of their PEG surfaces, nonassociation with culture medium protein was observed. These NPs were isolated and highly adhered to the cell surface, probably via RGD peptide–integrin interaction. This observation indicates that these types of NPs can be used to label receptors on the cell membrane to be visualized by SEM. In conclusion, AuNPs protected with tiopronin induce either endocytosis or adhesion to the cell membrane, depending on the chemical composition of the NP surface [51].

For cancer therapies that involve DNA–drug interactions, genes, short interfering RNA or antisense strategies that target RNA splicing, the nucleus is undoubtedly the target of interest; however, therapeutic agents must meet several requirements. A cell-specific nuclear probe must satisfy the following requirements:

- It must be small enough to enter cells and cross the nuclear membrane (<100 nm for uptake by receptor-mediated endocytosis [RME] and <30 nm for import through nuclear pores)
- Penetrate cellular membranes or bind to cell-specific plasma membrane receptors
- Bypass or escape endosomal/lysosomal pathways
- Penetrate nuclear membranes or access importins to pass through the nuclear pore complex
- Have low toxicity

A study in this field compared a 20-nm AuNP modified with distinct nuclear-localization peptides and evaluated cellular trajectories of peptide–AuNP complexes in the following three cell lines: HeLa, 3T3/NIH and Hep G2 [64]. These lines were chosen to illustrate cell-specific differences in nuclear targeting for each peptide studied. AuNPs were modified with four peptides: M1 (CGGGPKKKRKVGG), a peptide with a nuclear-localization signal derived from the T large

Figure 9. Effect in cell morphology of fibroblasts incubated with nanoparticles.

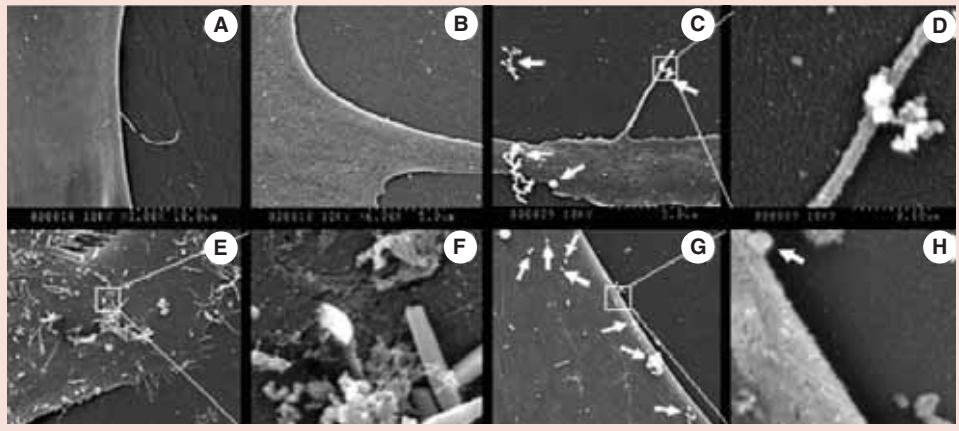

Scanning electron micoscope images of **(A & B)** control cells, **(C & D)** cells incubated with Au nanoparticle (NP)–tiopronin–RGD, **(E & F)** AuNP–tiopronin–ethylenediamine (EDA)–RGD and **(G & H)** AuNP–tiopronin–poly(ethylene glycol) (PEG)–RGD; white arrows show NP location. Large aggregates with few isolated AuNPs are observed in **(C & D)**. Formation of many lamellipodia and filopodia projecting from the cellular membrane was observed in cells treated with AuNP–tiopronin–EDA–RGD, while AuNP–tiopronin–PEG–RGD was attached at the cell membranes. Reproduced with permission from [51].

antigen of the SV-40 virus; M2 (CGGRKKRRQRRRAP), a peptide derived from the HIV Tat protein; M3 (CGGFSTSLRARKA), an adenovirus fiber protein; and M4 (CKKKKKKGGRGDMFG), which contains only the integrin-binding domain and a segment of six basic lysine residues [64]. Cellular trajectories of the peptides revealed a strong dependence on the cell line and type of peptide (Figure 10). M1 NPs entered all the cell lines, but there was little or no nuclear transport of these particles. M3 NPs entered the HeLa cell, escaped endosomes and passed through the nuclear pore complex; however, in 3T3/NIH cells, these particles clustered in endosomes and, in HepG2 cells, no uptake of M3 NPs was observed. The synthetic peptide M4 was the only one with the capacity to target the nucleus of HepG2 cells. Finally, M2 NPs did not enter any of the three cell lines, even though M2 contains the arginine-rich sequence of the Tfr24 peptide from the HIV Tat protein, which binds tightly to cell membranes.

On the basis of existing knowledge of protein structure and amino acid side chain packing/bonding properties, Levy and colleagues designed a peptide called CALNN, which self-assembled into a dense layer that excludes water. The Cys, which has a strong affinity for Au (because of the presence of a S atom that binds spontaneously to the Au surface), was incorporated at the N-terminal position of the sequence to anchor the peptide to the AuNP. Thus, CALNN-capped AuNPs can be freeze-dried and stored as powder for further use and, when redissolved in water, they maintain the same UV-vis absorption spectrum as before freeze-drying. The introduction of a specific recognition group on the AuNP surface is a simple strategy to achieve specific recognition of distinct motifs in a bioanalytical assay. In the same study, Levy and colleagues prepared NPs functionalized with biotin, as well as particles modified with a peptide analogue of biotin, Strep-tag II (WSHPQFEK). AuNPs were conjugated using a peptide mixture containing mainly CALNN and, in lesser proportions, CALNNG–KbiotinG or CALNNGG–strep–tag. To detect the presence of biotin and its peptide analogue, a streptactin peroxidase was used; a recombinant protein containing strep-tag was used as a positive control and CALNN–AuNP conjugates were used as controls for nonspecific interactions. AuNPs functionalized with biotin and a peptide analogue of biotin specifically interacted with streptavidin peroxidase [48].

Similarly, this research group also prepared peptide-capped AuNPs with another two biomolecular recognition sites expressed on their surface. They used CALNN pentapeptide, which provides a fast and simple approach to DNA functionalization, in order to obtain bifunctional NPs carrying both DNA and biotin moieties. These motifs were readily incorporated in a single stabilization–functionalization step via the

Figure 10. M1 Au nanoparticles incubated with HeLa cells.

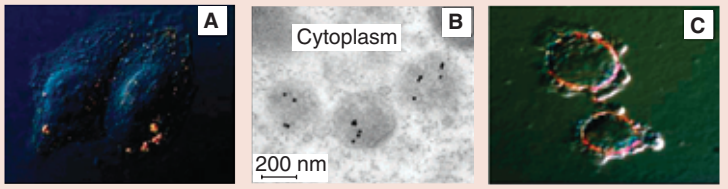

After 1 h, NPs were observed by **(A)** video-enhanced color differential interference contrast microscopy and **(B)** transmission electron microscopy in the cytoplasm. **(C)** NPs accumulated around the nuclear membrane after 2 h Reproduced with permission from [64]. ©2004, American Chemical Society.

CALNN peptide. AuNPs were prepared via citrate reduction, and were stabilized and functionalized by adding an aqueous mixture of the CALNN–DNA (18-base recognition sequence) and CALNNGK (biotin) G conjugates. To demonstrate the binding specificity of these bifunctional NPs, the researchers prepared two experiments: a protein microarray containing spots with avidin and control spots with protein A; and a DNA microarray containing spots with complementary DNA and control spots with DNA possessing mismatches of one, two and three bases. The results of specific binding of the bifunctional NPs to these microarrays showed that these particles bound to both avidin and complementary DNA with high specificity [49].

Another study with the CALNN peptide, developed by Wang and colleagues, is based on a colorimetric assay for kinase inhibitors by replacing the natural substrate of the kinase by functionalized AuNPs [50]. The synthesized 13-nm AuNPs were stabilized by the CALNN peptide and additionally modified with two further oligopeptide sequences: CALNN–AALRRASLG and CALNN–AAKKL-NRTLSVA. These sequences are known substrates of the cAMP-dependent protein kinase A (PKA) and the calmodulin-dependent kinase (CaM K)II, respectively. AuNP–peptide conjugates were incubated with either PKA or CaM-II, both in the presence of γ-biotin–ATP as a cosubstrate. The phosphorylation reaction resulted in the biotinylation of AuNPs. The conjugates were then mixed in solution with avidin-modified particles and, as a result of specific binding between biotin–avidin, aggregates formed. A change of color from red to blue indicated kinase-catalyzed biotinylation of substrate particles, while no change in color indicated efficient inhibition of the kinase reaction (Figure 11) [50].

Furthermore, the same authors also developed a route to protein-like metal NPs based on self-assembled peptide monolayers [72]. To separate peptide-capped NPs with a distinct number of molecular labels, these authors reported an immobilized metal ion affinity chromatography (IMAC) method for the purification of recombinant proteins. AuNPs were conjugated with a mixture of CALNN peptide and a functional peptide with two distinct entities: a His-tag (a sequence of six histidines), which is used due to its capacity to bind to immobilize chelated transition metal ions such as nickel, followed by a label (Gly–Lys–biotin–Gly), which could be any water-soluble molecular label, for instance, any peptide. The reaction of a mixture of CALNN and functional peptides resulted in populations of NPs bearing varying numbers of labels. IMAC is based on the separation of labeled NPs carrying one or more functional peptides from unlabeled NPs with no functional peptide. The mixture of labeled and unlabeled particles is applied to the IMAC gel and the immobilized Ni–nitrilotriacetic complex (Ni–NTA) specifically binds with His–Tag on the labeled NPs. Therefore the unlabeled NPs can be washed off. Finally, labeled NPs are eluted using imidazole as a competitor. Experiments showed that IMAC differentiates between NPs with none and one or more labels. This finding indicates that this sensitive method can be used for all types of nanomaterial capped with a peptide shell [72].

Recently, a study on neurodegenerative diseases, which are characterized by spontaneous self-assembly of proteins into insoluble fibrous deposits, has reported NP-mediated heating to dissolve amyloid deposits of $A\beta_{1-42}$ [47], a small protein involved in Alzheimer's disease (AD). These deposits were remotely and locally dissolved through the combined use of weak microwave fields and AuNPs. These AuNPs were linked to the peptide Cys–PEP, which has the capacity to selectively recognize Aβ aggregates, thereby forming the conjugate AuNP–Cys–PEP. The conjugate was incubated with a solution of $A\beta_{1-42}$, in which fibrils spontaneously started growing and forming precipitates. At a range of times and growth stages, a weak microwave field (0.1 W) was applied. The AuNP–Cys–PEP conjugate bound the fibrils, absorbed the radiation and dissipated energy, thereby causing the disaggregation of the amyloid deposits and aggregates (Figure 12). This disaggregation led to the formation of smaller species and amorphous aggregates. These findings were supported by TEM images of the aggregates before and after the irradiation, by thioflavin T assay and by size-exclusion chromatography analysis. These methods showed an

Figure 11. Section of a multiwell microplate containing substrate Au nanoparticles and six combinations (columns 1–3) of three potential inhibitors and two kinases (calmodulin-dependent kinase II and protein kinase A) after addition of avidin-modified nanoparticles.

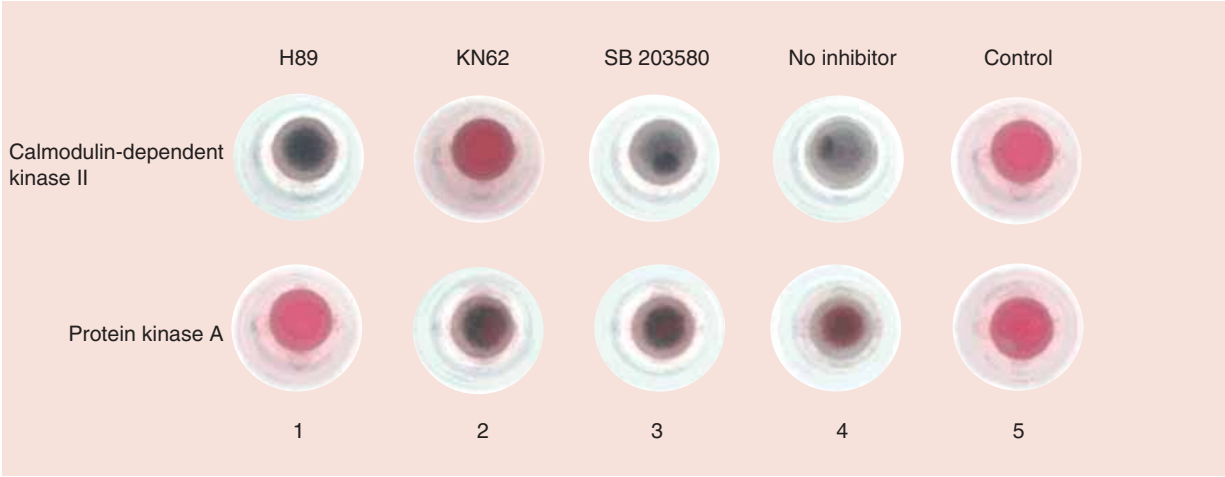

Control experiments were carried out in the absence of inhibitor (column 4) and in the absence of kinase (column 5). Red indicates no aggregation of particles (i.e., effective inhibition of the respective kinase), while dark blue/gray indicates aggregation (i.e., effective phosphorylation/biotinylation by the respective kinase).
Reproduced with permission from [50].

increment of low-molecular-weight species, such as monomers and oligomers. This in agreement with the conversion of high-molecular-weight aggregates to more soluble low-molecular-weight species during irradiation. Alternatively, the control ($A\beta_{1-42}$ alone incubated for 48 h and irradiated for 8 h) samples did not show the same effect [47].

In the field of enzymology, AuNPs can be used in a simple assay that allows the visual detection of a protease. This method, which is based on the aggregation of AuNPs when a AuNP colloid is treated with dithiols, allows the observation of a color change from pink to violet-blue since this band is shifted to a longer wavelength when clustering of colloid occurs. As thiols interact strongly with AuNPs, citrate-stabilized AuNPs were treated with a peptide of general formula Cys–$(AA)_n$–Cys and the color of the solution turned from pink-red to violet-blue. However, when AuNPs were treated with a peptide lacking a terminal Cys, no change in color was observed. Thus, the cleavage of a Cys–$(AA)_n$–Cys peptide in two fragments, each with a single Cys, does not induce aggregation of AuNPs. This observation was applied to design an assay for the qualitative detection of proteases, because the two Cys-containing peptides can be selectively recognized and cleaved by a specific protease. The authors synthesized a heptapeptide (Ac–Cys[Ac]–Gly–Dphe–Pro–Arg–Gly–Cys[Ac]–OH) as a substrate for thrombin, a serine protease involved in hemostasis. Treatment of the AuNP colloid with the heptapeptide caused the solution to turn from pink-red to blue. However, when an aliquot of solution resulting from the reaction of the peptide with thrombin was added to the Au colloid, no change in color was observed. This lack of change is attributed to the complete hydrolysis of the peptide, thereby obtaining two proteolytic fragments Ac–Cys(Ac)–Gly–Dphe–Pro–Arg–OH and H–Gly–Cys(Ac)–OH. The measure of absorbance at 600 nm, which is an indication of the formation of the cluster, allowed the authors to quantitatively follow the hydrolysis catalyzed by thrombin. Finally, the authors demonstrated that NP-based assays could be used for the preliminary analysis of biological fluids [73].

Mo and colleagues demonstrated the potential of NP-labeling techniques in detecting structurally unstable domains in collagen fibers, which are related to many debilitating human diseases [74]. They showed for the first time that a biochemically inert but highly helicogenic cartilage matrix protein (CMP; Pro–Hyp–Gly)$_7$ (Hyp = hydroxyproline), binds preferentially to the gap regions on the surface of intact type I collagen fibers. This binding behavior was demonstrated by synthesizing CMP conjugated to AuNPs of distinct sizes (NP-3 and -4) (Figure 13) that are colloidally stable under a wide range of aqueous conditions, and by TEM observation of their attraction to type I collagen fibers under physiological conditions

Figure 12. Transmission electron micrographs of the solutions before and after irradiation.

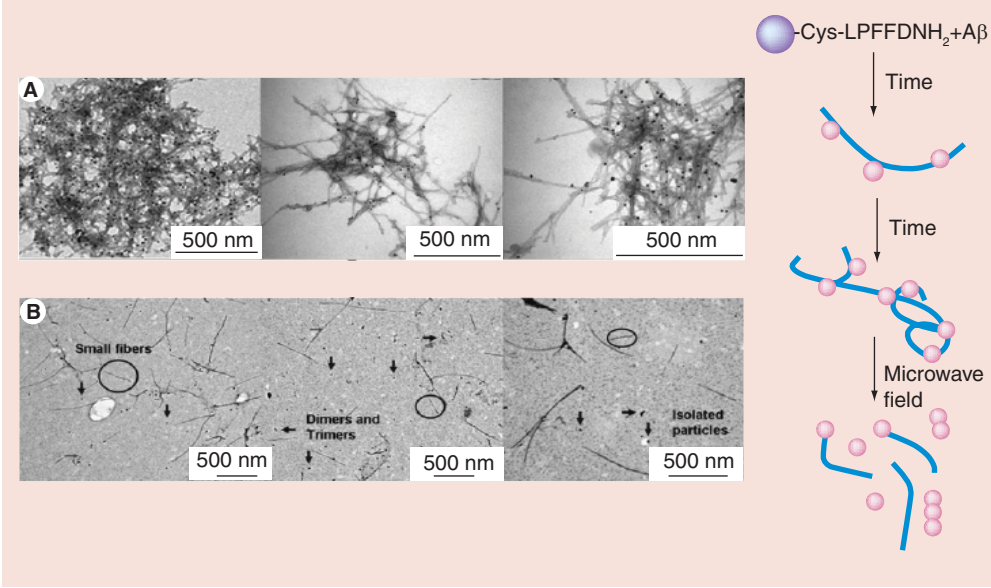

(A) Images of the AuNP–Cys–PEP bound to $A\beta_{1-42}$ aggregates after incubation of AuNP–Cys–PEP with 10-µM $A\beta_{1-42}$ for 48 h. **(B)** Images of the previous AuNP–Cys–PEP bound to $A\beta_{1-42}$ after 8 h of irradiation. Horizontal arrows indicate the presence of dimers and trimers, vertical arrows indicate the presence of isolated particles and circles indicate the presence of small fibers.
Reproduced with permission from [47]. ©2006, American Chemical Society.

(Figure 13). The authors claimed that the results suggested that this binding affinity is present in other natural proteins/peptides that hold collagen-like sequences [75].

Biomedical applications of peptide-IONP conjugates

IONPs have magnetic properties and offer many advantages. They can be used as contrasting agents in the field of magnetic resonance imaging (MRI) since the inclusion of magnetic particles within tissues allows a very large signal to be obtained from an MRI scanner. As IONPs travel through the bloodstream, they can increase the contrast signal and, hence, allow the study of a broad range of biological targets. The main requirement for MRI is the efficient capture of the magnetic NPs by the cell and, when a cell is sufficiently loaded with magnetic material, MRI can also be used for cell tracking [76,77]. Surface modification of superparamagnetic contrast agents with the HIV-1 Tat peptide is an effective technique for intracellular magnetic labeling because the conjugation of the Tat peptide to NPs facilitates their cellular uptake [78]. In addition, cells labeled with these conjugates can be readily detected by MRI.

Recently, ultrasmall superparamagnetic IO (USPIO) NPs have been conjugated to the HIV Tat peptide to label $CD4^+$ T cells for MRI. USPIO NPs were prepared for conjugation of the Tat peptide by functionalization to the dextran that covers the magnetic NP surface [79]. Two USPIO-functionalized NPs were obtained. In the first, the mean valence (number of Tat peptide molecules per NP) of the NPs was estimated to be 15 and, in the second, it was 45. The uptake and loading of the USPIO NPs in $CD4^+$ T cells was examined using inductively coupled plasma optical emission spectrometry (ICP-OES), a technique that allows measurement of the Fe content of treated cells. A concentration-dependent increase in cell labeling was observed when Tat-derivatized NPs were used in a 5-min reaction, with no uptake of Fe when unconjugated USPIO NPs were used. The NPs with increased valence labeled over 95% of T cells within 5 min, whereas those with a lower valence (i.e., only 15) achieved a labeling efficiency of 20–40%. Furthermore, the authors of the study demonstrated that labeled $CD4^+$ T cells retained their proliferative and regulatory function *in vitro* and, similarly, no differences were observed in their transmigratory behavior. The imaging potential of this contrast

Figure 13. Transmission electron microscopy micrographs.

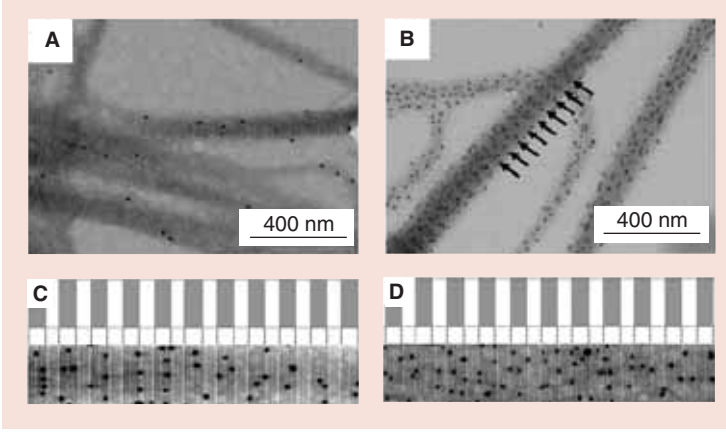

Reconstituted type I collagen fibers after incubation with **(A)** NP-4 (particle size = 16.2 ± 3.1 nm) and **(B–D)** NP-3 (26.9 ± 4.6 nm) functionalized with cartilage matrix protein. Functionalized NP-4 NPs show little affinity for collagen fibers. By contrast, NP-3 shows strong affinity for collagen fibers. Binding occurred preferentially to the dark bands (arrows in **(B)** and gray boxes in **(C)**) of collagen fibers when the experiment was performed at 25°C. **(D)** There was no such preference when the collagen fibers and NP-3 were incubated at 40°C and cooled to room temperature.
Reproduced with permission from [74].

agent for MRI was measured, and Tat USPIO–NPs provided effective contrast enhancement *in vitro*, while the unlabeled cells did not yield any contrast. Moreover, cell viability was reduced at high concentrations of Tat–USPIO NPs. Above 50%, cell death was visible by light microscopy 1 h after incubation with the highest concentration assayed.

Another study in the same field addressed the feasibility of using MRI to monitor T cells *in vivo* after loading the cells with monocrystalline superparamagnetic IONPs modified with a peptide sequence from the Tat protein of HIV-1. The Tat peptide sequence was conjugated to a small IO (5 nm) core coated with cross-linked (CL) aminated dextran, thereby yielding CLIO–Tat NPs. The Tat peptide was modified to carry a fluorescein isothiocyanate (FITC) tag in order to follow the peptide during conjugation and as a marker for fluorescence microscopy. This study showed that the presence of FITC-conjugated CLIO–Tat in T cells was dose dependent, that is, 97% of cells were FITC-positive after loading with 8000 ng/ml of FITC–CLIO–Tat NPs. Confocal microscopy images of labeled cells showed strong FITC staining in most of the loaded T cells (>95%). The FITC label was distributed in clusters throughout the cytoplasm and nuclei. Moreover, there was no alteration in the cells' cytoplasmic or nuclear morphology, as shown by confocal microscopy. Analysis of apoptosis by flow cytometry revealed that the FITC–CLIO–Tat conjugate did not increase the percentage of apoptotic cells compared with unloaded T cells. This study also examined whether loading of T cells with FITC–CLIO–Tat NPs interfered with cell functions. The results indicated that labeling of T cells with more than 8000 ng/ml of magnetic NPs did not affect activation, proliferation or upregulation functions. Finally, to measure the effects of T cells labeled with Tat peptide-derived NPs on the spleen by MRI, a group of six B6 mice were injected intravenously with a suspension of T cells loaded with 8000 ng/ml of FITC–CLIO–Tat. Changes in image intensity caused by the agent were measured by MRI, thereby proving that these particles can be used to analyze T-cell distribution events *in vivo* [52,80]. In addition, superparamagnetic NPs of maghemite (γ-Fe_2O_3) have been conjugated to another peptide as potent intracellular carriers for a molecular MRI diagnosis agent. NPs were prepared by a chemical coprecipitation method, encapsulated with an Arg-containing cell-penetrating peptide (RRRRRRRRCK–FITC) and conjugated with poly (D, L lactide-co-glycolide) (PLGA) (Figure 14). The FITC was conjugated to observe the intracellular translocation of magnetic NPs into human mesenchymal stem cells, and cellular internalization was examined using a confocal laser scanning microscope (CLSM). Cells were incubated with γ-Fe_2O_3–PLGA–Arg–FITC NPs for 2–18 h. Particles were effectively adsorbed onto the membrane of stem cells (Figure 15). The cytotoxicity of this intracellular carrier was checked using an MTT and lactate dehydrogenase release assay. Cell incubation with NP–peptide conjugates did not show significant cytotoxicity up to 200 µg/ml of IONP concentrations [81].

A method to detect Aβ plaques in the brain of transgenic mice that overexpress amyloid precursor protein (APP) or both mutant APP and presenilin (PS)-1 by micro-MRI has also been reported [82]. This procedure uses the $A\beta_{1–40}$ peptide magnetically labeled with monocrystalline IONPs (MIONs). Dextran-coated MION particles were linked to the $A\beta_{1–40}$ peptide to asses their capacity to bind $A\beta_{1–42}$ peptide, the major constituent of AD plaque amyloid. In an *in vivo* assay, the magnetically labeled peptides were coinjected with mannitol, an agent to increase blood–brain barrier (BBB) permeability. This preparation was injected directly into

Figure 14. Preparation of γ-Fe_2O_3–PLGA–Arg–FITC nanoparticles.

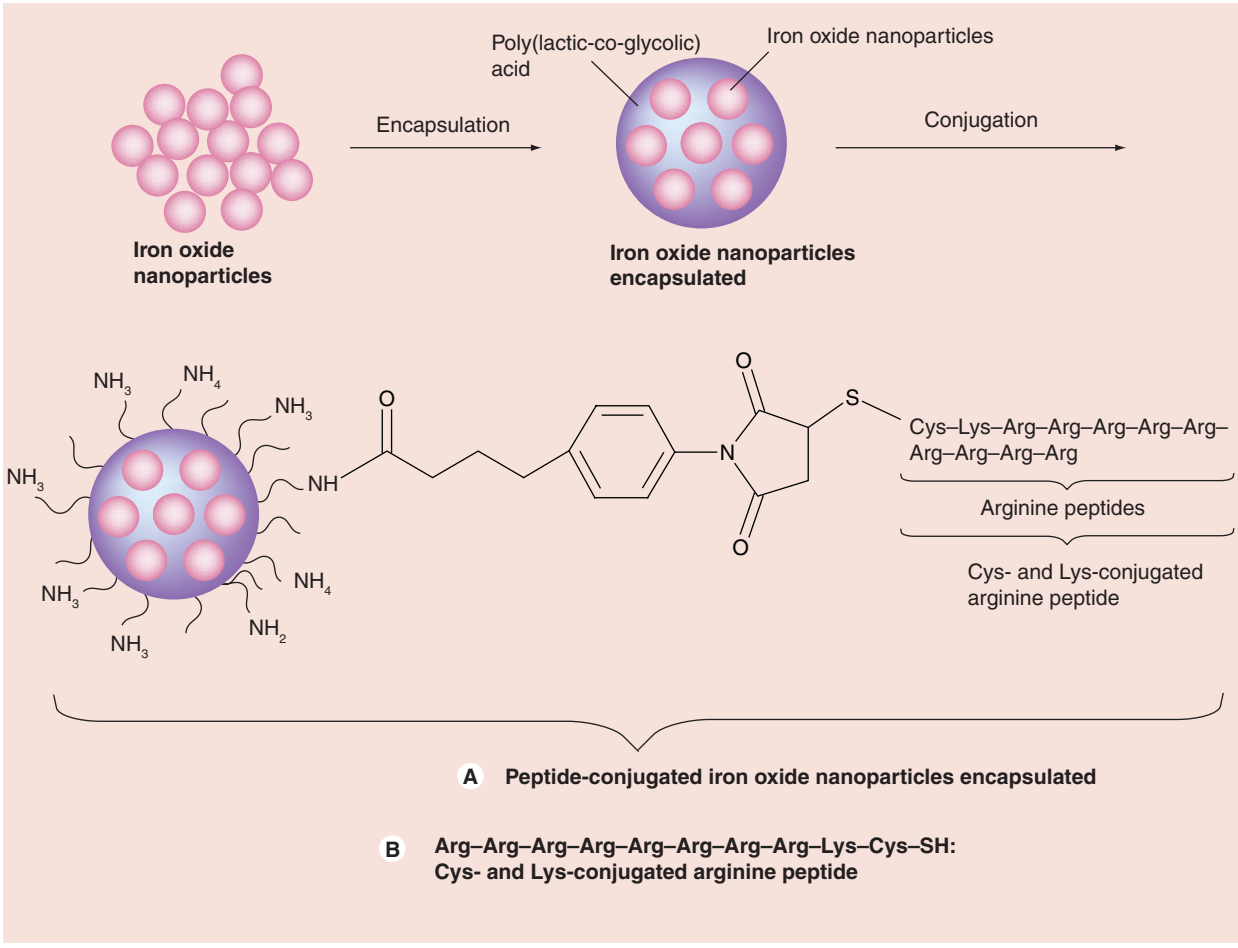

Reproduced with permission from [81]. ©2005, American Institute of Physics.

the common carotid artery of AD transgenic mice and nontransgenic controls. The systemic injection of $A\beta_{1–40}$ peptide adsorbed onto MION particles with mannitol detected Aβ plaques by micro-MRI in the brain of AD transgenic mice. This study showed that $A\beta_{1–40}$ peptide, in this case, is essential for targeting to Aβ plaques, because, when the MION particles were injected alone in transgenic mice, plaques were not detected.

Biomedical applications of peptide–Co NP conjugates

Thanh and colleagues were the first to report the use of peptides as capping ligands for *in situ* synthesis of water-soluble CoNPs with the aim to apply these particles for biological purposes [83]. The peptide TLVNN facilitates the formation of NPs and partly protects these particles from oxidation. Furthermore, a recently described elegant application is the use of peptides to control the nucleation and growth of inorganic NPs *in vitro*. The authors identified a unique set of sequences that bind to Ag and CoNPs from a phage peptide display library using a polymerase chain reaction (PCR)-driven method. The peptides identified by the method described in this study also work as templates for the synthesis of Ag and Co platinum NPs [84].

Conclusion

In this review, we have discussed the current use of peptides conjugated to metallic NPs in bioresearch and, to a limited extent, in biomedicine. In addition, the preparation and characterization of the conjugates have been examined. Characterization of the conjugates involves the standard techniques used for peptides and NPs. However, other techniques remain to be examined for a more complete characterization, that is, methods that allow determination of the secondary structure of the

Figure 15. Image of stem cells after incubation with the γ-Fe_2O_3–PLGA–Arg–FITC nanoparticles.

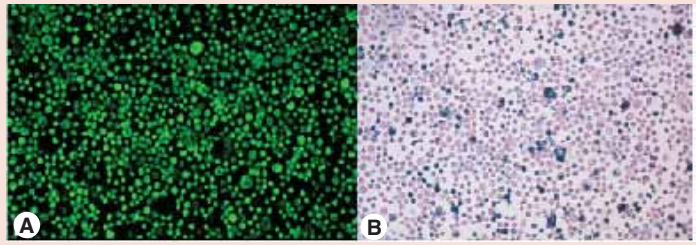

(A) Confocal laser scanning microscopy image of stem cells after incubation with γ-Fe_2O_3 –PLGA–Arg–FITC nanoparticles (NPs) at 37°C for 2 h. **(B)** The optical microscope image for Prussian blue staining with γ-Fe_2O_3 –PLGA–Arg–FITC NPs.
Reproduced with permission from [81]. ©2005.

peptides anchored to the NPs. Furthermore, one of the main concerns is how peptides interact and pack on a NP surface. Our group is currently conducting research in this regard. This information could improve our understanding of the contribution of the peptide to biocompatibility and also of the biological recognition of NPs to the target.

We have also discussed the advantages of peptides in increasing the stability, biocompatibility and tagging of NPs. However, it is important to point out that few toxicity studies have been performed. To date, cytotoxicity tests are not complete in terms of assessing the effects of nanomaterials on cellular metabolism. MTT and cell viability assays are not sufficient and a more thorough approach is required. Peptides that offer a wide range of therapeutic properties, together with metallic NPs that present properties of interest, create new avenues for the design of novel biomedical strategies.

Future perspective

The applications of metallic NPs in new therapeutic strategies are promising. However, several concerns, such as toxicity, stability and tagging,

Executive summary

Preparation of AuNPs & IONPs

- Au nanoparticle (NP) size can be controlled by changing the $HAuCl_4$:citrate ratio. However, iron oxide (IO)NPs (either Fe_3O_4 [magnetite] or γ-Fe_2O_3 [maghemite]) can be synthesized through the coprecipitation of Fe^{2+} and Fe^{3+} aqueous salt solutions by the addition of a base. Organized assemblies or complex structures have been used as reactors to obtain ultrafine magnetic IONPs.

Peptide synthesis

- Although several methodologies have been described for peptide synthesis, the one of choice for the preparation of peptides linked to NPs is the solid-phase technique.

Preparation of peptide–metallic NP conjugates

- Two main strategies to bind peptides to AuNPs have been reported. In strategy A, the conjugation of a peptide with biological activity to a AuNP is via the spontaneous reaction of a thiol, present in a Cys moiety belonging to the peptide sequence, with the AuNP surface. By contrast, in strategy B, a functionalized NP is capped with a linker, which is then activated and functionalized with the biologically active peptide. In the case of IONPs, they are first stabilized with an adsorbed layer of a biocompatible polymer, such as dextran or polymetacrylate, and the peptide is then conjugated with the biocompatible NP.

Characterization of peptide–metal NP conjugates

- The characterization of conjugated peptide–AuNPs requires the use of combined techniques.

Biomedical applications of peptide–AuNP conjugates

- Peptide–AuNP conjugates have potential applications in cancer and Alzheimer´s disease therapy and diagnosis. Furthermore, capping AuNPs with peptides increases stability and biocompatibility and allows them to be directed to the desired target.
- Applications of metallic NPs conjugated to peptides in new therapeutic strategies are promising. However, several concerns, such as toxicity, stability and tagging, must be addressed.
- In the field of enzymology, peptide–AuNPs can be used in a simple assay that allows the visual detection of a protease.

Biomedical applications of peptide–IONP conjugates

- Peptides conjugated to IONPs can be used as contrasting agents in the field of magnetic resonance imaging. Surface modification of superparamagnetic IONP contrast agents with peptides is an effective technique for intracellular magnetic labeling.

Biomedical applications of peptide–CoNP conjugates

- Peptides are used as capping ligands for *in situ* synthesis of water-soluble Co NPs with the aim to apply these particles for biological purposes.

must be addressed. Also, a field of debate is the mechanism of NP delivery to the cell. From our point of view, the cellular uptake and targeting of NPs could be improved using peptide carriers that have the capacity to cross the cell membrane, thereby allowing the NPs to target the cellular compartment of interest. The success of particle development and the application of these particles in clinical and biological laboratories requires an interdisciplinary focus. Collaboration in the fields of materials science, chemistry, magnetic characterization, cell engineering and testing, as well as clinical trials, is one of the great challenges of this line of research.

Acknowledgements

Work in our laboratories was partially supported by: Chile – FONDAP 11980002, FONDECYT 1061142, FONDECYT 7060219; Spain – CICYT (CTQ2006–03794/BQU), ISCIII (CIBER, nanomedicine), the Generalitat de Catalunya (2005SGR 00662), the Institute for Research in Biomedicine and the Barcelona Science Park. MK and FA give special thanks to AECI for providing a Chile–Spain collaboration grant.

Bibliography

Papers of special note have been highlighted as either of interest (•) or of considerable interest (••) to readers.

1. Pankhurst QA, Connolly J, Jones SK *et al.*: Applications of magnetic NPs in biomedicine. *J. Phys. D Appl. Phys.* 36, R167–R181 (2003).
2. Huh YM, Jun YW, Song HT *et al.*: *In vivo* magnetic resonance detection of cancer by using multifunctional magnetic nanocrystals. *J. Am. Chem. Soc.* 127, 12387–12391 (2005).
3. Loo Ch, Lowery A, Halas N *et al.*: Immunotargeted nanoshells for integrated cancer imaging and therapy. *Nano Lett.* 5(4), 709–711 (2005).
4. Efremov RG, Chugunov AO, Pyrkov TV *et al.*: Molecular lipophilicity in protein modeling and drug design. *Curr. Med. Chem.*14(4), 393–415 (2007).
5. Naz RK, Dabir P: Peptide vaccines against cancer, infectious diseases, and conception. *Front. Biosci.* 12, 1833–1844 (2007).
6. Cruz LJ, Iglesias E, Aguilar JC *et al.*: Different immune response of mice immunized with conjugates containing multiple copies of either consensus or mixotope versions of the V3 loop peptide from human immunodeficiency virus type 1. *Bioconjug. Chem.* 15, 1110–1117 (2004).
7. Daniel MC, Astruc D: AuNPs: assembly, supramolecular chemistry, quantum-size-related properties, and applications toward biology, catalysis, and nanotechnology. *Chem. Rev.* 104(1), 293–346 (2004).

• Complete review related to the synthesis and characterization of Au nanoparticles (NPs).

8. Turkevich J, Stevenson PC, Hillier J: A study of the nucleation and growth processes in the synthesis of colloidal gold. *Discuss. Faraday Soc.* 11, 55–75 (1951).
9. Frens G: Controlled nucleation for the regulation of the particle size in monodisperse gold suspensions. *Nat. Phys. Sci.* 241, 20–22 (1973).
10. Zhang LX, Sun XP, Song YH, Jiang X, Dong SJ, Wang EA: Didodecyldimethylammonium bromide lipid bilayer-protected gold nanoparticles: synthesis, characterization, and self-assembly. *Langmuir* 22(6), 2838–2843 (2006).
11. Huang CJ, Chiu PH, Wang YH, Chen KL, Linn JJ, Yang CF: Electrochemically controlling the size of AuNPs. *J. Electrochem. Soc.* 153(12), D193–D198 (2006).
12. Goodman CM, McCusker CD, Yilmaz T, Rotello VM: Toxicity of AuNPs functionalized with cationic and anionic side chains. *Bioconjug. Chem.* 15(4), 897–900 (2004).
13. Busbee BD, Obare SO, Murphy CJ: An improved synthesis of high-aspect-ratio gold nanorods. *Adv. Mater.* 15(5), 414–416 (2003).
14. Doolittle JW, Dutta PK: Influence of microwave radiation on the growth of AuNPs and microporous zincophosphates in a reverse micellar system. *Langmuir* 22(10), 4825–4831 (2006).
15. Shen M, Du YK, Hua NP, Yang P: Microwave irradiation synthesis and self-assembly of alkylamine-stabilized AuNPs. *Powder Technol.* 162(1), 64–72 (2006).
16. Mafune F, Kohno JY, Takeda Y, Kondow T: Full physical preparation of size-selected gold nanoparticles in solution: laser ablation and laser-induced size control. *J. Phys. Chem. B* 106(31), 7575–7577 (2002).
17. Bjerneld EJ, Svedberg F, Kall M: Laser-induced growth and deposition of noble-metal NPs for surface-enhanced Raman scattering. *Nano Lett.* 3(5), 593–596 (2003).
18. Park JE, Atobe M, Fuchigami T: Synthesis of multiple shapes of AuNPs with controlled sizes in aqueous solution using ultrasound. *Ultrason. Sonochem.* 13(3), 237–241 (2006).
19. Okitsu K, Ashokkumar M, Grieser F: Sonochemical synthesis of AuNPs: effects of ultrasound frequency. *J. Phys. Chem. B* 109(44), 20673–20675 (2005).
20. Su CH, Wu PL, Yeh CS: Sonochemical synthesis of well-dispersed AuNPs at the ice temperature. *J. Phys. Chem. B* 107(51), 14240–14243 (2003).
21. Yang YC, Wang CH, Hwu YK, Je JH: Synchrotron x-ray synthesis of colloidal gold particles for drug delivery. *Mat. Chem. Phys.* 100(1), 72–76 (2006).
22. Seino S, Kinoshita T, Otome Y *et al.*: γ-ray synthesis of composite NPs of noble metals and magnetic iron oxides. *Scripta. Mater.* 51(6), 467–472 (2004).
23. Karadas F, Ertas G, Ozkaraoglu E, Suzer S: X-ray-induced production of AuNPs on a SiO_2/Si System and in a poly(methyl methacrylate) matrix. *Langmuir* 21(1), 437–442 (2005).
24. Gachard E, Remita E, Khatouri J, Keita B, Nadjo L, Belloni J: Radiation-induced and chemical formation of gold clusters. *N. J. Chem.* 22(11), 1257–1265 (1998).
25. Kabashin AV, Meunier M: Laser ablation-based synthesis of functionalized colloidal nanomaterials in biocompatible solutions. *J. Photochem. Photobiol. A* 182(3), 330–334 (2006).
26. Andreescu D, Sau TK, Goia DV: Stabilizer-free nanosize gold sols. *J. Colloid Interface Sci.* 298(2), 742–751 (2006).
27. Gupta AK, Gupta M: Synthesis and surface engineering of iron oxide NPs for biomedical applications. *Biomaterials* 26(18), 3995–4021 (2005).

• Complete review related to the synthesis and characterization of iron oxide (IO)NPs.

28. Reimers GW, Khalafalla SE: Preparing magneticfluids by a peptizing method. *US Bureau Mines Tech. Rep.* 59 (1972)
29. Hadjipanayis GC, Siegel RW: Nanophase materials: synthesis, properties and applications. *NATO ASI series Appl. Sci.* E260, Kluwer, Dordrecht, The Netherlands (1993).
30. Sjogren CE, Briley-Saebo K, Hanson M, Johansson C: Magnetic characterization of iron oxides for magnetic resonance imaging. *Magn. Reson. Med.* 31(3), 268–272 (1994).
31. Collier JH, Messersmith PB: Biomimetic mineralization, mesoporous structures. In: *Encyclopedia of Materials: Science and Technology.* Buschow KH, Buschow J, Cahn RW *et al.* (Eds). Elsevier Science, Amsterdam, Holland 602–606 (2001).
32. Sinha A, Das SK, Rao V, Ramachandrarao P: Synthesis of organized inorganic crystal assemblies. *Curr. Sci.* 79(5), 646–648 (2000).
33. Rosensweig RE: *Ferrohydrodynamics.* Rosensweig RE (Ed.). Dover Publications INC Cambridge University Press, New York, NY, USA (1985).
34. Tillotson TM, Gash AE, Simpson RL, Hrubesh LW, Satcher JH: Nanostructured energetic materials using sol–gel methodologies. *J. Noncryst. Solids* 285, 335–358 (2001).
35. Ziolo RF, Giannelis EP, Weinstein BA *et al.*: Matrix mediated synthesis of γ-Fe_2O_3: a new optically transparent magnetic material. *Science* 257, 219–223 (1992).
36. Deng Y, Wang L, Yang W, Fu S, Elaiessari A: Preparation of magnetic polymeric particles via inverse microemulsion polymerization process. *J. Magn. Magn. Mater.* 257(1), 69–78 (2003).
37. Santra S, Tapec R, Theodoropoulou N, Dobson J, Hebard A, Tan W: Synthesis and characterization of silica-coated iron oxide NPs in microemulsion: the effect of non-ionic surfactants. *Langmuir* 17, 2900–2906 (2001).
38. Li S, Irwin G, Simmons B, John V, McPherson G, Bose A: Structured materials synthesis in a self-assembled surfactant mesophase. *Colloids Surf. A* 174, 275 (2000).
39. Lloyd-Williams P, Albericio F, Giralt E: *Chemical Approaches to the Synthesis of Peptides and Proteins.* Albericio F (Ed.). CRC, Boca Raton, FL, USA (1997).
- Pedagogic book related to peptide synthesis.
40. Merrifield, Bruce R: Solid-phase synthesis (Nobel lecture). *Angew. Chem.* 97, 801–812 (1985).
41. Albericio F, Chinchilla R, Dodsworth DJ *et al.*: New trends in peptide coupling reagents. *Org. Prep. Proced. Int.* 33(3), 203–303 (2001).
42. Kaiser E, Colescott RL, Bossinger CD *et al.*: Color test for detection of free terminal amino groups in the solid-phase synthesis of peptides. *Anal. Biochem.* 34(2), 595–598 (1970).
43. Chan WC, White PD: *Fmoc Solid Phase Peptide Synthesis.* Oxford University Press, Oxford, UK 303–327 (2000).
44. Albericio F: Orthogonal protecting groups for Nα-amino and C-terminal carboxyl functions in solid-phase peptide synthesis. *Biopolymers* 55, 123–139 (2000).
45. Selsted ME: HPLC methods for purification of antimicrobial peptides. *Methods Mol. Biol.* 78, 17–33 (1997).
46. Yeganeh MS, Dougal SM, Polizzotti RS, Rabinowitz P: Interfacial atomic structure of a self-assembled alkyl thiol monolayer /Au (111): a sum-frequency generation study. *Phys. Rev. Lett.* 74, 1811–1814 (1995).
47. Kogan MJ, Bastus NJ, Amigo R *et al.*: NP-mediated local and remote manipulation of protein aggregation. *Nano Lett.* 6, 110–115 (2006).
- Interesting potential application of a conjugated peptide–AuNP for the treatment of Alzheimer's disease.
48. Levy R, Thanh TK, Doty RC *et al.*: Rational and combinatorial design of peptide capping ligands for AuNPs. *J. Am. Chem. Soc.* 126, 10076–10084 (2004).
- One of the pioneer works related to the potential use and properties of peptides–AuNPs.
49. Wang Z, Lévy R, Fernig DG, Brust M: The peptide route to multifunctional AuNPs. *Bioconjug. Chem.* 16, 497–500 (2005).
50. Wang Z, Lévy R, Fernig DG, Brust M: Kinase-catalyzed modification of AuNPs: a new approach to colorimetric kinase activity screening. *J. Am. Chem. Soc.* 128, 2214–2215 (2006).
51. De la Fuente JM, Berry CC, Riehle MO, Curtis SG: NPs targeting at cells. *Langmuir* 22, 3286–3293 (2006).
52. Josephson L, Tung CH, Moore A, Weissleder R: High-efficiency intracellular magnetic labelling with novel superparamagnetic–Tat peptide conjugates. *Bioconjug. Chem.* 10, 186–191 (1999).
53. Lewin M, Carlesso N, Tung CH *et al.*: Tat peptide-derivatized magnetic NPs allow *in vivo* tracking and recovery of progenitor cells. *Nat. Biotechnol.* 18, 410–414 (2000).
54. Bhadriraju K, Hansen LK: Hepatocyte adhesion, growth and differentiated function on RGD-containing proteins. *Biomaterials* 21(3), 267–272 (2000).
55. Meriaudeau F, Downey T, Wig A *et al.*: Fiber optic sensor based on gold island plasmon resonance. *Sens. Actuators B* 54(1), 106–117 (1999).
56. Mie G: Contributions to the optics of turbid media, especially colloidal metal solutions. *Ann. Physik.* 25, 377 (1908).
57. Kreibig U, Genzel L: Optical absorption of small metallic nanoparticles. *Surf. Sci.* 156, 678 (1985).
58. Creighton JA, Eadon DG: Ultraviolet-visible absorption spectra of the colloidal metallic elements. *Faraday Trans. J. Chem. Soc.* 87, 3881 (1991).
59. Link S, El-Sayed M: Spectral propierties and relaxation dynamics of surface plasmon electronic oscillations in gold and silver nanodots and nanorods. *J. Phys. Chem. B* 103(40), 8410–8426 (1999).
60. Link S, Mohamed MB, El-Sayed M: Simulation of the optical absorption spectra of gold nanorods as a function of their aspect ratio and the effect of the medium dielectric constant. *J. Phys. Chem. B* 103, 3073–3077 (1999).
61. Shipway AN, Lahav M, Gabai R *et al.*: Investigations into the electrostatically induced aggregation of gold nanoparticles. *Langmuir* 16(23), 8789–8795 (2000).
62. Mandal TK, Si S: pH-controlled reversible assembly of peptide-functionalized gold nanoparticles. *Langmuir* 23, 190–195 (2007).
63. De la Fuente JM, Berry CC: Tat peptide as an efficient molecule to translocate AuNPs into the cell nucleus. *Bioconjug. Chem.* 16, 1176–1180 (2005).
- Nice example of how a peptide could contribute to the translocation of AuNPs.
64. Tkachenko AG, Xie H, Liu Y *et al.*: Cellular trajectories of peptide-modified gold NP complexes: comparison of nuclear localization signals and peptide transduction domain. *Bioconjug. Chem.* 15, 482–490 (2004).
65. Tkachenko AG, Xie H, Coleman D *et al.*: Multifunctional gold nanoparticles–peptide complexes for nuclear targeting. *J. Am. Chem. Soc.* 125, 4700–47701 (2003).
66. Baudhuin P, Beauvois S, Courtoy PJ: *Colloidal Gold: Principles, Methods, and Applications.* Hayat MA (Ed.). Academic Press, New York, NY, USA (1989).

67. Fabris L, Antonello S, Armelao L *et al.*: Gold nanoclusters protected by conformationally constrained peptides. *J. Am. Chem. Soc.* 128, 326–336 (2006).
68. Hostetler MJ, Wingate JE, Zhong CJ *et al.*: Alkanethiolate gold cluster molecules with core diameters from 1.5 to 5.2 nm: core and monolayer properties as a function of core size. *Langmuir* 14, 17–30 (1998).
69. Bourg MC, Badia A, Lennox RB: Gold sulfur bonding in 2D and 3D self-assembled monolayers: XPS characterization. *J. Phys. Chem.* 104, 6562–6567 (2000).
70. Jain PK, Lee KS, El-Sayed IH *et al.*: Calculated absorption and scattering properties of AuNPs of different size, shape, and composition: applications in biological imaging and biomedicine. *J. Phys. Chem. B* 110(14), 7238–7248 (2006).
71. Slocik JM, Stone MO, Naik RR: Synthesis of gold nanoparticles using multifunctional peptides. *Small* 1(11), 1048–1052 (2005).
72. Lévy R, Wang Z, Duchesne L *et al.*: A generic approach to monofunctionalized protein-like AuNPs based on immobilized metal ion affinity chromatography. *Chembiochem* 7, 592–594 (2006).
73. Guarise C, Pasquato L, De Filippis V, Scrimin P: AuNPs-based proteasa assay. *Proc. Natl Acad. Sci. USA* 103, 3978–3982 (2006).
74. Mo X, An Y, Yun Ch-S, Yu MS: Nanoparticle-assisted visualization of binding interactions between collagen mimetic peptide and collagen fibers. *Angew. Chem. Int. Ed.* 45, 2267–2270 (2005).
75. Shaw LM, Olsen BR: FACIT collagens: diverse molecular bridges in extracellular matrices. *Trends Biochem. Sci.* 16, 191 (1991).
76. Berry CC, Curtis SG: Functionalisation of magnetic NPs for application in biomedicine. *J. Phys. D Appl. Phys.* 36, R198–R206 (2003).
77. Hernando A, Crespo P, García MA: Metallic magnetic NPs. *Scientific Worldjournal* 5, 972–1001 (2005).
78. Zhao M, Kircher MF, Josephson L, Weissleder R: Differential conjugation of Tat peptide to superparamagnetic NPs and its effect on cellular uptake. *Bioconjug. Chem.* 13, 840–844 (2002).
79. Garden OA, Reynolds PR, Yates J *et al.*: A rapid method for labelling $CD4^+$ T cells with ultrasmall paramagnetic iron oxide NPs for magnetic resonance imaging that preserves proliferative, regulatory and migratory behaviour *in vitro*. *J. Inmunol. Methods* 314, 123–133 (2006).
80. Dodd CH, Hsu HC, Chu WJ *et al.*: Normal T cell response and *in vivo* magnetic resonance imaging of T cells loaded with HIV transactivator-peptide-derived superparamagnetic NPs. *J. Immunol. Methods* 256, 89–105 (2001).
81. Lee SJ, Jeong JR, Shin SC *et al.*: Intracellular translocation of superparamagnetic iron oxide NPs encapsulated with peptide-conjugated poly(D,L lactide-co-glycolide). *J. Appl. Phys.* 97, 10Q913–1 (2005).
82. Wadghiri YZ, Sigurdsson EM, Sadowski M *et al.*: Detection of Alzheimer's amyloid in transgenic mice using magnetic resonance microimaging. *Magn. Reson. Med.* 50, 293–302 (2003).
83. Thanh TK, Puntes VF, Tung LD, Fernig DG: Peptides as capping ligands for *in situ* synthesis of water solubles Co NPs for bioapplications. *J. Phys. Conf. Series* 17, 70–76 (2005).
84. Naik RR, Jones SE, Murray CJ *et al.*: Peptide templates for NP synthesis derived from polymerase chain reaction-driven phage display. *Adv. Funct. Mater.* 1, 25–30 (2004).